SCIENCE CHINA
Chemistry

• ARTICLES •

December 2012 Vol.55 No.12: 2587–2594
doi: 10.1007/s11426-012-4797-1

Molecular dynamics study on the relationships of modeling, structural and energy properties with sensitivity for RDX-based PBXs

XIAO JiJun[1,2*], ZHAO Li[1], ZHU Wei[3], CHEN Jun[4], JI GuangFu[4], ZHAO Feng[4], WU Qiang[4] & XIAO HeMing[1*]

[1]*Molecule and Material Computation Institute, Nanjing University of Science and Technology, Nanjing 210094, China*
[2]*State Key Laboratory of Explosion Science and Technology, Beijing Institute of Technology, Beijing 100081, China*
[3]*College of Biological, Chemical Sciences and Engineering, Jiaxing University, Jiaxing 314001, China*
[4]*National Key Laboratory of Shock Wave and Detonation Physics, Institute of Fluid Physics, China Academy of Engineering Physics, Mianyang 621900, China*

Received July 11, 2012; accepted August 17, 2012; published online November 15, 2012

In this paper, a primary model is established for MD (molecular dynamics) simulation for the PBXs (polymer-bonded explosives) with RDX (cyclotrimethylene trinitramine) as base explosive and PS as polymer binder. A series of results from the MD simulation are compared between two PBX models, which are represented by PBX1 and PBX2, respectively, including one PS molecular chain having 46 repeating units and two PS molecular chains with each having 23 repeating units. It has been found that their structural, interaction energy and mechanical properties are basically consistent between the two models. A systematic MD study for the PBX2 is performed under NPT conditions at five different temperatures, i.e., 195 K, 245 K, 295 K, 345 K, and 395 K. We have found that with the temperature increase, the maximum bond length (L_{max}) of RDX N–N trigger bond increases, and the interaction energy ($E_{N\text{-}N}$) between two N atoms of the N–N trigger bond and the cohesive energy density (CED) decrease. These phenomena agree with the experimental fact that the PBX becomes more sensitive as the temperature increases. Therefore, we propose to use the maximum bond length L_{max} of the trigger bond of the easily decomposed and exploded component and the interaction energy $E_{N\text{-}N}$ of the two relevant atoms as theoretical criteria to judge or predict the relative degree of heat and impact sensitivity for the energetic composites such as PBXs and solid propellants.

RDX (cyclotrimethylene trinitramine), PBXs (polymer-bonded explosives), molecular dynamics (MD) simulation, sensitivity, trigger bond length, interaction energy, cohesive energy density (CED)

1 Introduction

RDX (cyclotrimethylene trinitramine) is a well-known highly energetic explosive and extensively used in the fields of defense, aerospace, and civil economy as an oxidant or solid filler in the formulations of polymer-bonded explosives (PBXs), booster explosives and solid propellants, as shown in Figure 1. It has been widely studied *via* experimental and theoretical methodologies for its structure, physical and chemical properties [1–13], among which [1–4] are mainly devoted to experiments, while [5–13] provide a number of theoretical results.

Sensitivity of energetic materials is defined as the degree to which they can be initiated to explode by external stimulus. Each of the stimuli, such as impact, heat, friction, shock wave and electric spark, corresponds to its specific sensitivity. The sensitivity of energetic materials is used as a measure of their safety and is one of the most significant properties that affect their production, storage and application, as

*Corresponding authors (email: xiao_jijun@yahoo.com.cn; xiao@mail.njust.edu.cn)

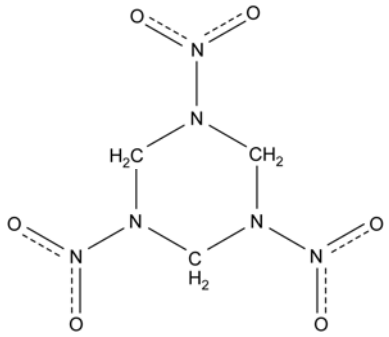

Figure 1 Chemical structure of RDX (cyclotrimethylene trinitramine).

well as the design of new energetic materials. For example, in the theoretical design of the currently most popular HEDMs (high energetic density materials), the sensitivity is one of the most important performances [14] under consideration.

Although the determination of the sensitivity mainly relies on experiments, it would be of great significance if the sensitivity can be predicted based on theoretical study. Up to present, theoretical study about sensitivity prediction only focuses on the molecules and crystals of energetic compounds. For example, based on the quantum chemistry calculation for the energetic compound molecules, these methods were proposed, such as oxygen balance OB_{100} [15], electrostatic potential [16], bond order [17], bond dissociation energy [18], activation energy [19, 20], charge distribution [21], as well as the recently presented artificial neural network [22, 23] and QSPR (quantitative structure-property relationship) [24, 25]. As for the energetic compound crystals, earlier studies are based on semi-empirical X_α and EHCO calculation, a principle of the easiest transition (PET) [26–28] that has ever been proposed, and recent results are the band gap criterion for the sensitivity and the review paper [29]. However, as for the energetic composites, to our best knowledge, only Refs. [30, 31] predict the heat and impact sensitivity with L_{max} of N–NO_2 trigger bond (the initial chemical bond fractured in decomposition and detonation under external stimuli) in the sensitive component HMX (cyclotetramethylene tetranitramine) for HMX/AP (NH_4ClO_4) two-constituent system.

In general, the base explosive added with a small amount of polymers which comprises PBX or propellant is necessary for practical use due to simple process, low sensitivity and good mechanical properties. Although many studies on the PBX safety have been conducted via experiments, few results are available concerning the theoretical criteria of its sensitivity up to now. Thus, it is significant to theoretically study the sensitivity for the PBX and search for effective theoretical criteria.

In this work, we study the practically used PBX based on RDX with PS as the polymer binder. We first introduce the force field and the model construction, followed by the MD simulation at different temperatures. The L_{max} of N–NO_2 trigger bond, the interaction energy $E_{N\text{-}N}$ among N atoms in the trigger bond, and the cohesive energy density (CED) are investigated and discussed in details, and in the meantime the theoretical criteria to predict the sensitivity are proposed at the first time.

2 Methods, modeling and computation

2.1 Force field

Classical molecular dynamics simulation is appropriate for studying the structure and property relationships for large and complicated systems such as PBXs, and it is able to provide statistical and average results approximately. We have used COMPASS force field to conduct classical MD simulation for PBXs and investigated their binding energy and mechanical properties [12, 32–34]. Later we studied the explosive, cohesive, and thermal properties under this force field, and applied them to the formulation design.

The COMPASS force field [35] adopts the framework of CFF-type force field [36, 37], and is especially suitable for studying condensed phase and interaction between different types of constituents. Its total energy is expressed as:

$$\begin{aligned}
E_{\text{total}} = & \sum_b [K_2(b-b_0)^2 + K_3(b-b_0)^3 + k_4(b-b_0)^4] \\
& + \sum_\theta [H_2(\theta-\theta_0)^2 + H_3(\theta-\theta_0)^3 + H_4(\theta-\theta_0)^3] \\
& + \sum_\varphi [V_1(1-\cos\varphi) + V_2(1-\cos 2\varphi) + V_3(1-\cos 3\varphi)] \\
& + \sum_\chi k_x(\chi-\chi_0)^2 + \sum_{b,b'} F_{b,b'}(b-b_0)(b'-b_0') \\
& + \sum_{b,\theta} F_{b\theta}(b-b_0)(\theta-\theta_0) \\
& + \sum_{b,\varphi} (b-b_0)[F_{b,\varphi}^{(1)}(1-\cos\varphi) + F_{b,\varphi}^{(2)}(1-2\cos\varphi) \\
& + F_{b,\varphi}^{(3)}(1-3\cos\varphi)] \\
& + \sum_{\theta,\theta'} F_{\theta,\theta'}(\theta-\theta_0)(\theta'-\theta_0') \\
& + \sum_{\theta,\theta',\varphi} F_{\theta,\theta',\varphi}(\theta-\theta_0)(\theta'-\theta_0')\cos\varphi \\
& + \sum_{i,j} \frac{q_i q_j}{\varepsilon_0 r_{i,j}} + \sum_{i,j} \varepsilon_{i,j} \left[2\left(\frac{r_{i,j}^0}{r_{i,j}}\right)^9 - 3\left(\frac{r_{i,j}^0}{r_{i,j}}\right)^6 \right]
\end{aligned} \tag{1}$$

This function can be divided into two categories: valence terms and nonbond interaction terms. The valence terms represent internal coordinates of bond (b), angle (θ), torsion angle (ϕ), out-of-plane angle (χ), and the cross-coupling terms including combinations of two or three internal coordinates. The nonbond interactions, which include a LJ-9-6 function [38] for van der Waals (vdW) term and a Coulombic function for an electrostatic interaction, are used for the interactions between pairs of atoms that are separated by two or more intervening atoms or those that belong to dif-

ferent molecules. q_i denotes the net charge for atom i, and $\varepsilon_{i,j}$, $r_{i,j}$ and $r^0_{i,j}$ are the LJ-9-6 parameters.

In this force field, the valence parameters and atomistic partial charges are derived by fitting to ab initio data, and the vdW parameters are derived by conducting MD simulations of molecular liquids and fitting the simulated cohesive energies and equilibrium densities to experimental data. The combined parameterization procedure significantly improves the quality of a general force field.

2.2 Modeling

Based on the initial RDX in Ref. [1], we cut along the (001) crystalline surface of its (2×3×4) crystal cell with Cartesian z axis parallel to lattice vector c and at the same time perpendicular to (001) crystalline surface. The vacuum layer height was set as zero and the area of (001) crystalline surface was equal to 23.15 × 32.13 Å^2. The RDX crystal primary cell containing 192 RDX molecules, corresponding to 4032 atoms, was then built and written as RDX(001).

For the establishment of a PBX primary cell with PS, the mass ratio RDX:PS ≈ 9:1 was used to be consistent with experiments. Thus, we used a PS molecular chain having 46 repeating units or two PS molecular chains with each having 23 repeating units, which are denoted as PS1 and PS2, respectively. The periodic cell containing the PS molecular chain was firstly built with the bottom plane having the same shape and size as (001) surface of RDX(001) and the c axis perpendicular to the bottom plane. A c value was set so that the periodic cell density was about half of the PS density. Gradually press c value and after each pressing, optimize the PS chain so that its total energy was minimized. This process continued until the cell density was about the same as the PS density. A PS periodic cell and a c value were obtained ultimately, and the c value is denoted as $\overline{c}$. Another RDX(001) periodic simulation cell was thus set up, but with the vacuum layer height set as $\overline{c}$. The PS molecular chain in the periodic cell was then put on the RDX(001) crystalline surface, and a PBX periodic cell, i.e. a PBX model, was thus established. It is correspondingly abbreviated as PBX1 with PS1 and PBX2 with PS2. Figure 2 shows the structures of RDX(001), PBX1 and PBX2 primary cells.

2.3 Computation

The above obtained RDX(001), PS1, PS2, PBX1 and PBX2 evolved dynamically in isothermal-isobaric (NPT) ensembles with Andersen temperature control [39] and Parrinello-Rahman pressure control [40]. The pressure was set as 0.0001 GPa. Five temperatures of 195, 245, 295, 345 and 395 K were considered. During the simulation, the van der Waals interactions were truncated at the radius of 9.5 Å, the electrostatic (Coulomb) interactions were calculated via the standard Ewald summation [41], and the equations of motion were integrated with a step of 1 fs. The equilibration runs of 0.5 ns duration were performed, followed by production runs of 1 ns, during which data were collected for subsequent analysis and the sampling interval was taken as 10 fs. The MD modeling and computations were carried out using software program-MS (Material Studio) from Accelrys Inc. (San Diego, CA).

Binding energy quantitatively represents the interaction strength of molecules. Higher binding energy means stronger interaction between constituents and thus more stable PBX. It has important influences on the compatibility, the mechanical and the explosive properties of energetic composites. The binding energy is calculated as:

$$E_{\text{bind}} = -E_{\text{inter}} = -(E_{\text{total}}-E_{\text{RDX}}-E_{\text{PS}}) \quad (2)$$

where E_{total}, E_{RDX} and E_{PS} respectively stand for the potential energies of the PBX, RDX and PS in the equilibrium system.

Next, we define the interaction energy $E_{\text{N-N}}$ between N

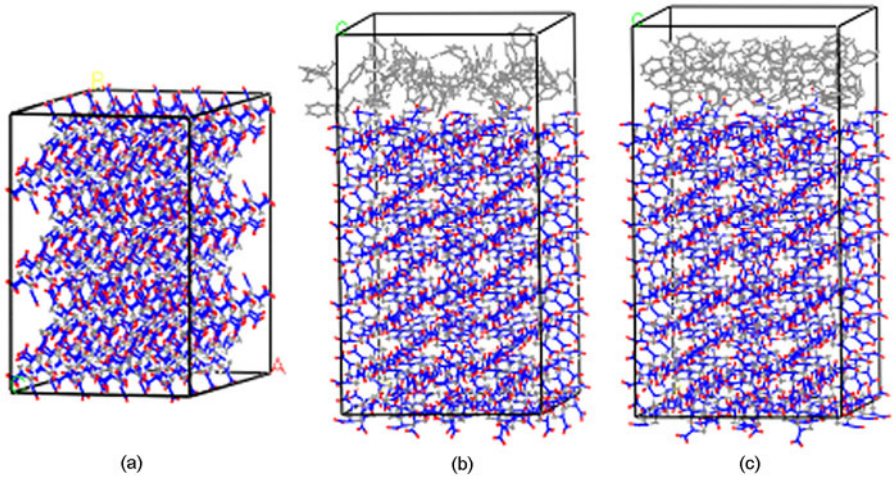

Figure 2 Primary cells of RDX(001) (a), PBX1 (b) and PBX2 (c).

and N atoms in N–NO_2 trigger bond as follows:

$$E_{N\text{-}N} = (E_{total}-E')/n \quad (3)$$

where E_{total} represents the total energy of the system, E' is the system energy with all N atoms fixed purposely, and n is the number of N–NO_2 trigger bonds. The $E_{N\text{-}N}$ value is actually one kind of difference value. Obviously, $E_{N\text{-}N}$ is a measure of N–N bond strength in the prescribed force filed framework as in Eq. (1). Higher $E_{N\text{-}N}$ means stronger N–N bond which is not easily to break, and thus the corresponding system is not sensitive.

All of the interaction energies presented in this paper were calculated by averaging over 10 equilibrium configurations in the trajectory, and these configurations are independent of each other, since the time interval between them is 100 ps and long enough.

The CED is the amount of intermolecular energy needed for a material to transfer from condensed phase to gas phase, i.e.,

$$CED = (\Delta H-RT)\times\rho/M \quad (4)$$

where ΔH is the heat of sublimation, M is the molecular weight, and ρ is the density. It is measurable *via* experiments. In atomistic simulations, it is defined as the increase of the energy per mole per unit volume of the material until all intermolecular forces are eliminated.

3 Results and discussion

3.1 Bond length, $E_{N\text{-}N}$ and mechanical properties of PBX1 and PBX2

Figure 3 shows the equilibrium structures of RDX(001), PBX1 and PBX2. The statistical distribution of N–NO_2 trigger bond length at the temperature 295 K was obtained and is shown in Figure 4. In RDX(001), 97% of the RDX molecules have bond length from 1.330 to 1.450 Å; in PBX1, 98% have bond length from 1.330 to 1.460 Å; and in PBX2, 97% have bond length from 1.330 to 1.452Å. The most probable bond length L_{prob}, the average bond length L_{ave}, and the maximum bond length L_{max} of N–NO_2 trigger bond are listed in Table 1. It is seen that both L_{prob} and L_{ave} are nearly the same for RDX(001), PBX1 and PBX2. Their average bond lengths L_{ave} are 1.389, 1.390 and 1.390 Å, respectively, and approximate to the experimental value 1.413 Å for RDX crystalline state [1]. The trigger bond length calculated by B3LYP/6-31*[6] in RDX gaseous state is 1.424 Å. In contrast to RDX(001), L_{max} of PBX1 and PBX2 is obviously increased due to the interfacial interaction between PS and RDX. They are respectively 1.590 Å and 1.592 Å, which are almost the same.

Table 2 gives $E_{N\text{-}N}$ data and its components for PBX1 and PBX2, which are found unchanged. Table 3 shows the mechanical properties such as tensile modulus, shear modulus, bulk modulus, and Poisson's ratio for PS1, PS2, PBX1, and PBX2. It is seen that for the two models, PBX1 and PBX2, the structure, energy and mechanical properties do not have much change. This means that either of the two models is suitable for searching for statistical regulations of the structure and properties through MD simulation. Therefore, we use PBX2 model to study the correlation of the structure and properties with the sensitivity as follows.

3.2 Relationship of L_{max} and sensitivity

Previous studies based on quantum chemical calculation proposed the principle of smallest bond order (PSBO) [17, 27]: for series of energetic compounds with similar molecular structure, smaller bond order of trigger bond in molecules means the compound is more sensitive, and the smallest bond order means the compound is the most sensitive. This principle has been used extensively in the prediction of impact sensitivity for various types of energetic compounds. Moreover, in reactive force fields, energies are built as

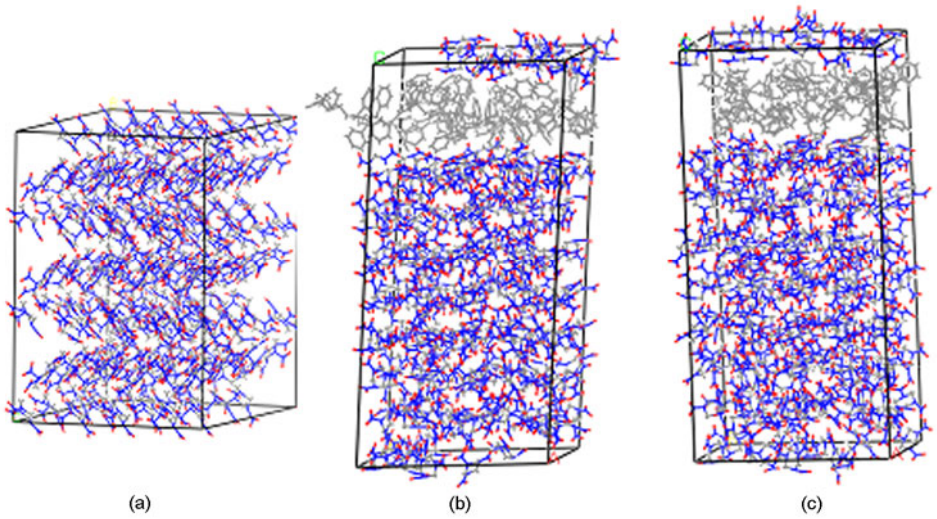

Figure 3 Equilibrium structures of RDX(001) (a), PBX1 (b) and PBX2 (c).

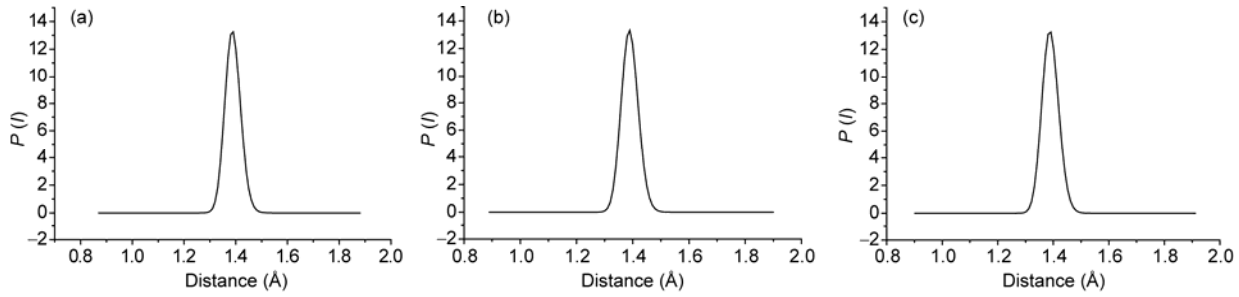

Figure 4 N–NO_2 trigger bond length distributions of RDX(001) (a), PBX1 (b) and PBX2 (c).

Table 1 L_{prob}, L_{ave} and L_{max} (Å) of N–NO_2 trigger bond in RDX(001), PBX1 and PBX2

	RDX(001)	PBX1	PBX2
L_{prob}	1.390	1.390	1.392
L_{ave}	1.389	1.390	1.390
L_{max}	1.570 (5.2×10^{-8}) [a]	1.590 (1.7×10^{-8}) [a]	1.592 (1.7×10^{-8}) [a]

a) Percentage of the molecules with L_{max}.

Table 2 E_{N-N} (kcal/mol) and relevant energies in PBX1 and PBX2 [a]

	PBX1	PBX2
E_{N-N}	41.5	41.5
Internal	0.3	0.3
Nonbond	41.1	41.1
vdW	–0.5	–0.5
Repulsive	1.4	1.5
Dispersive	–1.9	–1.9
Electrostatic	41.7	41.6

a) $E_{N-N} = E$(Internal) + E(Nonbond); E(Nonbond) = E(vdW)(E(Repulsive) + E(Dispersive)) + E(Electrostatic).

Table 3 Mechanical properties (GPa) of PS1, PS2, PBX1 and PBX2

	PS1	PS2	PBX1	PBX2
Tensile modulus E	1.4	1.8	3.7	3.0
Poisson's ratio γ	0.4	0.4	0.3	0.4
Bulk modulus K	2.4	2.6	3.4	4.1
Shear modulus G	0.5	0.6	1.4	1.1

functions of bond order. Classical MD simulation does not involve electronic structure, and cannot give the bond order data. However, it is able to give statistical distribution of the bond length, as shown in Figure 4. Usually, for chemical bonds in molecules, higher bond order corresponds to shorter bond length, and vice versa. Politzer *et al.* [42] have used the reciprocals of the lengths of the N–NO_2 and C–NO_2 bonds to measure the bond strength and described the impact sensitivity of nitramine and nitro compounds.

Table 4 shows the data of L_{ave} and L_{max} of the trigger bond N–NO_2 in PBX2. As the temperature increases, L_{ave} does not change much, while L_{max} increases monotonously and significantly, although the percentage of the molecules with L_{max} (10^{-8} as seen in the bracket) is very small. As the temperature increases, the molecular movement becomes faster, and the atoms away from the equilibrium position vibrate higher, leading to longer bond length. The minority of the molecules with L_{max} is activated and tends to induce decomposition and explosion, which thereby makes the sensitivity become higher as the temperature increases. In Refs. [30, 31], the trigger bond L_{max} of HMX was used to correlate with the heat and impact sensitivity of HMX/AP composite and the obtained results for different ratios and temperatures agree well with the experimental results. Here, the trigger bond L_{max} of RDX is firstly involved in the sensitivity prediction for RDX crystal and its PBXs, and is shown to be suitable as a theoretical criterion for the heat and impact sensitivity.

3.3 Relationship of interaction energy and sensitivity

3.3.1 Binding energy E_{bind}

Table 5 shows E_{bind} of PBX2 as well as E_{total}, E_{PS}, and E_{RDX} at different temperatures. The change of E_{bind} with temperature is shown in Figure 5. It is observed that E_{bind} decreases rapidly and to a minimum point at 295 K, and goes up as the temperature increases, and then goes down slightly as the temperature increases further. This complicated change is understandable, as E_{bind} is affected by many factors and only

Table 4 L_{ave} and L_{max} (Å)of N–NO_2 in PBX2 at different temperatures

	195 K	245 K	295 K	345 K	395 K
L_{ave}	1.388	1.389	1.390	1.391	1.391
L_{max}	1.542 (1.7×10^{-8}) [a]	1.561 (3.5×10^{-8}) [a]	1.592 (1.7×10^{-8}) [a]	1.614 (3.5×10^{-8}) [a]	1.624 (3.5×10^{-8}) [a]

a) Percentage of the molecules with L_{max}.

Table 5 E_{bind} (kcal/mol) of PBX2 at different temperatures

T (K)	E_{total}	E_{PS}	E_{RDX}	E_{bind}
195	–52641.9	196.8	–52427.3	411.4
245	–51778.3	308.9	–51726.3	360.9
295	–51040.5	421.6	–51132.7	329.4
345	–50181.7	531.3	–50370.3	342.6
395	–49175.3	636.6	–49470.9	341.0

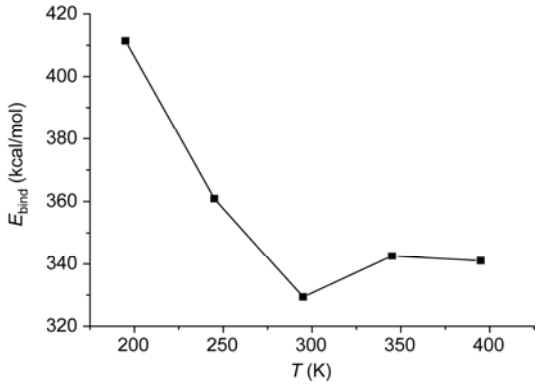

Figure 5 E_{bind} versus temperature of PBX2.

characterizes the entire thermal stability of the system, whereas the sensitivity acts within "hot spot" theory as a local property. Thus, the binding energy cannot be used to predict the sensitivity.

3.3.2 *Atom interaction energy $E_{N–N}$*

Table 6 shows the interaction energy $E_{N–N}$ of N atoms in the N–NO_2 trigger bond at different temperatures and other component energies. The change of $E_{N–N}$ with the temperature is visibly shown in Figure 6. It is noticed that $E_{N–N}$ decreases monotonously with the temperature increasing. Less $E_{N–N}$ means that the material is more sensitive, which agrees with the fact that materials are more sensitive with a higher temperature. This is easily understood, as less energy is required to separate two N atoms connected by the trigger bond at a higher temperature, and the system is more easily to decompose and explode, i.e., more sensitive. Overall, $E_{N–N}$ can be used as a theoretical criterion to predict the heat and impact sensitivity of the PBX. Also from Table 6, $E_{N–N}$ approximates to the nonbond energy under COMPASS force field, which is mainly due to the electrostatic energy and small portion of vdW.

3.3.3 *Cohesive energy density CED*

The cohesive energy densities (CEDs) are listed in Table 7, and shown in Figure 7. Under COMPASS force field for MD simulation, CED is actually a nonbond energy between molecules, i.e., the sum of vdW and electrostatic energy.

As seen in Table 7 and Figure 7, with the temperature increasing, CED, vdW, and electrostatic energy all decrease monotonously. This agrees with the experimental fact that the sensitivity becomes higher with the temperature increasing, as lower energy needed for the material to transfer from the condensed phase to gas phase tends to cause decomposition and explosion, leading to higher sensitivity. Therefore, CED can also be used as a theoretical criterion for the heat and impact sensitivity.

Table 6 $E_{N–N}$ (kcal/mol) and relevant energies in PBX2 at different temperatures [a)]

	195 K	245 K	295 K	345 K	395 K
$E_{N–N}$	42.1	41.6	41.5	40.7	40.3
Internal	0.2	0.3	0.3	0.4	0.4
Nonbond	41.8	41.3	41.1	40.3	39.9
vdW	–0.5	–0.5	–0.5	–0.5	–0.5
Repulsive	1.5	1.5	1.5	1.3	1.1
Dispersive	–2.0	–2.0	-1.9	–1.8	–1.6
Electrostatic	42.3	41.8	41.6	40.8	40.5

a) E_{N-N} = E(Internal) + E(Nonbond); E(Nonbond) = E(vdW)(E(Repulsive) + E(Dispersive))+ E(Electrostatic).

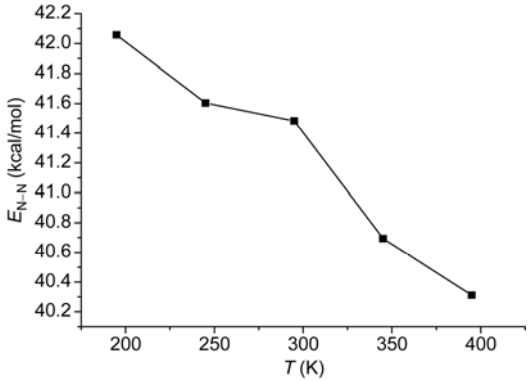

Figure 6 E_{N-N} versus temperature of PBX2.

Table 7 Cohesive energy density CED (kcal/cm^3) and relevant energies of PBX2 at different temperatures [a)]

	195 K	245 K	295 K	345 K	395 K
CED	0.21	0.20	0.19	0.18	0.16
vdW	0.08	0.08	0.08	0.07	0.07
Electrostatic	0.13	0.12	0.11	0.11	0.10

a) CED = E(vdW) + E(Electrostatic).

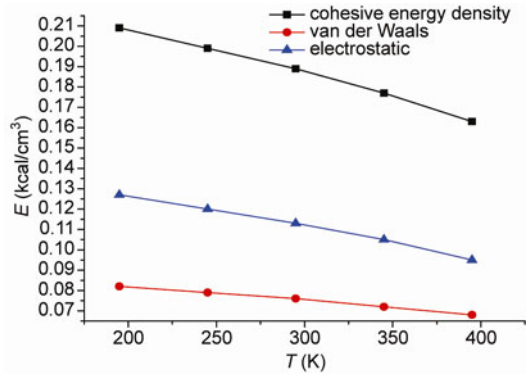

Figure 7 CED, vdW, and electrostatic versus temperature of PBX2.

4 Conclusions

The structure and the energy properties of RDX crystal and its PBXs with PS as the binder have been studied through MD atomistic simulation. The conclusions have been drawn as follows:

(1) Two PBX models separately having one PS chain with 46 units and two PS chains with each having 23 units have been considered. MD simulation has shown similar structure, energy, and mechanical properties, which implies that the two models are both applicable in terms of the study on structure and properties via MD simulation.

(2) The $N–NO_2$ trigger bond length distribution of RDX and its PBX has been obtained, and the average bond length L_{ave} approximates to the experimental bond length. The maximum bond length L_{max} increases monotonously with higher temperature, which is consistent with the experimental fact of the increasing sensitivity. The trigger bond L_{max} is thus found to be an effective structure factor that can be used to judge the heat and impact sensitivity.

(3) Binding energy characterizes the thermal stability of the whole system, and is not so related to the local property, sensitivity. As a measure of N–N bond strength, the interaction energy $E_{N\text{-}N}$ among N atoms in $N–NO_2$ trigger bond decreases as the temperature increases. Thus, it can be used as a theoretical criterion to predict the heat and impact sensitivity of the PBX.

(4) The cohesive energy density CED decreases with the temperature increasing which means less energy needed to transfer from condensed phase to gas phase, leading to easier decomposition and explosion, and higher sensitivity.

This work was financially supported by the National Key Laboratory of Shock Wave and Detonation Physics, Institute of Fluid Physics, China Academy of Engineering Physics (076100-1197F), the Defence Industrial Technology Development Program (B1520110002) and the State Key Laboratory of Explosion Science and Technology, Beijing Institute of Technology (KFJJ09-5).

1 Choi CS, Prince E. The crystal structure of cyclotrimethylenetrinitramine. *Acta Cryst*, 1972, B28: 2857–2862
2 Kishore K. Thermal decomposition studies on hexahydro-1,3,5-trinitro-s-triazine (RDX) by differential scanning calorimetry. *Propell Explos Pyrotech*, 1977, 2: 78–81
3 Schwarz RB, Hooks DE, Dick JJ, Archuleta JI, Martinez AR. Resonant ultrasound spectroscopy measurement of the elastic constants of cyclotrimethylene trinitramine. *J Appl Phys*, 2005, 98: 056106–056108
4 Haycraft JJ, Stevens LL, Eckhardt CJ. The elastic constants and related properties of the energetic material cyclotrimethylene trinitramine (RDX) determined by Brillouin scattering. *J Chem Phys*, 2006, 124: 024712-1–024712-11
5 Sorescu DC, Rice BM, Thompson DL. Intermolecular potential for the Hexahydro-1,3,5-trinitro-1,3,5-s-triazine crystal (RDX): A crystal packing, Monte Carlo, and molecular dynamics study. *J Phys Chem*, 1997, B101: 798–808
6 Xiao JJ, Ji GF, Yang D, Xiao HM. The DFT studies on structure and property of hexahydro-1,3,5-trinitro-2,4,6-triazine. *Chin J Struct Chem*, 2002, 21: 437–441
7 Swell TD, Bennett C*M*. *Monte Carl*o calculations of the elastic moduli and pressure-volume-temperature equation of state for hexahydro-1,3,5-trinitro-1,3,5-triazine. *J Appl Phys*, 2000, 88: 88–95
8 Strachan A, Kober E, van Duin ACT, Oxgaard J, Goddard III WA. Thermal decomposition of RDX from reactive molecular dynamics. *J Chem Phys*, 2005, 122: 054502-1–054502-10
9 Boyd S, Gravelle M, Politzer P. Nonreactive molecular dynamics force field for crystalline hexahydro-1,3,5-trinitro-1,3,5 triazine. *J Chem Phys*, 2006, 124: 104508-1–104508-10
10 Zheng L, Thompson DL. Molecular dynamics simulations of melting of perfect crystalline hexahydro-1,3,5-trinitro-1,3,5-*s*-triazine. *J Chem Phys*, 2006, 125: 084505-1–084505-9
11 Agrawal PM, Rice BM, Zheng L, Thompson DL. Molecular dynamics simulations of hexahydro-1,3,5-trinitro-1,3,5-*s*-triazine (RDX) using a combined Sorescu-Rice-Thompson AMBER force field. *J Phys Chem*, 2006, B110**:** 26185–26188
12 Zhu W, Xiao JJ, Zhu WH, and Xiao HM. Molecular dynamics simulations of RDX and RDX-based plastic-bonded explosives. *J Hazards Mater*, 2009, 164: 1082–1088
13 Zhou TT, Huang FL. Effects of defects on thermal decomposition of HMX *via* ReaxFF molecular dynamics simulations. *J Phys Chem*, 2011, B115: 278–287
14 Xiao HM, Xu XJ, Qiu L. *Theoretical Design of High Energy Density Materials*. Beijing: Science Press, 2008
15 Kamlet MJ, Adolph HG. The relationship of impact sensitivity with structure of organic high explosives. *Propell Explos Pyrotech,* 1979, 4: 30–34
16 Politzer P, Abrahmsen L, Sjoberg P. Effects of amino and nitro substituents upon the electrostatic potential of an aromatic ring. *J Am Chem Soc*, 1984, 106: 855–860
17 Xiao HM, Wang ZY, Yao JM. Quantum chemical study on sensitivity and stability of aromatic nitro explosives I. Nitro derivatives of aminobenzenes. *Acta Chim Sinica*, 1985, 43: 14–18
18 Politzer P, Murray JS. Relationships between dissociation energies and electrostatic potentials of $C–NO_2$ bonds: Applications to impact sensitivities. *J Mol Struct*, 1996, 376: 419-424
19 Fan JF, Xiao HM. Theoretical study on pyrolysis and sensitivity of energetic compounds. (2) Nitro-derivatives of benzene. *J Mol Struct (Theochem)*, 1996, 365: 225–229
20 Chen ZX, Xiao HM, Yang SL. Theoretical investigation on the impact sensitivity of tetrazolederivatives and their metal salts. *Chem Phys*, 1999, 250: 243–248
21 Rice BM, Hare JJ. A quantum mechanical investigation of the relation between impact sensitivity and the charge distribution in energetic molecules. *J Phys Chem*, 2002, A106: 1770–1783
22 Keshavarz MH. Prediction of impact sensitivity of nitroaliphatic, nitroaliphatic containing other functional groups and nitrate explosives. *J Hazards Mater*, 2007, 148: 648–652
23 Keshavarz MH, Jaafari M. Investigation of the various structure parameters for predicting impact sensitivity of energetic molecules *via* artificial neural network. *Propell Explos Pyrotech*, 2006, 31: 216–225
24 Benazet S, Jacob G, Pepe G. GenMol(TM) supramolecular descriptors predicting reliable sensitivity of energetic compounds. *Propell Explos Pyrotech*, 2009, 34: 120–135
25 Wang R, Jiang J, Pan Y, Cao H, Cui Y. Prediction of impact sensitivity of nitro energetic compounds by neural network based on electrotopological-state indices. *J Hazards Mater*, 2009, 166: 155–186
26 Xiao HM, Li YF, Qian JJ. A study on sensitivity and conductivity of alkali and heavy metal azides. *Acta Phys Chim Sinica*, 1994, 10: 235–240
27 Xiao HM, Li YF. Banding and electronic-structures of metal azides-sensitivity and conductivity. *Science in China (Series B)*, 1995, 38: 538–545
28 Xiao HM, Li YF. *Banding and Electronic Structures of Metal Azides-Sensitivity and Conductivity*. Beijing: Science Press, 1996
29 Zhu WH, Xiao HM. First-principles band gap criterion for impact sensitivity of energetic crystals: A review. *Struct Chem*, 2010, 21: 657–665

30 Zhu W, Xiao JJ, Zheng J, Zhao XB, Chen ZE, Xiao HM. A theoretical criterion for sensitivity of energetic composites–molecular dynamics studies on AP/HMX systems at various concentrations and temperatures. *Acta Chim Sinica*, 2008, 66: 2592–2596
31 Zhu W, Wang XJ, Xiao JJ, Zhu WH, Sun H, Xiao HM. Molecular dynamics simulations of AP/HMX composite with a modified force field. *J Hazards Mater*, 2009, 167: 810–816
32 Xiao JJ, Ma XF, Zhu W, Xiao HM. Molecular dynamics simulations of polymer bonded-explosives (PBXs): Modeling, elastic properties and their dependence on temperatures and concentrations of binders. In: *Proceedings of the eighth seminar "New trends in research of energetic materials"*. Pardubice: The University of Pardubice, 2005. 19–21
33 Xu XJ, Xiao HM, Xiao JJ, Zhu W, Huang H, Li JS. Molecular dynamics simulations for pure ε-CL-20 and ε -CL-20-based PBXs. *J Phys Chem*. 2006, B110: 7203–7207
34 Qiu L, Xiao HM, Zhu WH, Xiao JJ, Zhu W. *Ab initio* and molecular dynamics studies of crystalline TNAD (trans-1,4,5,8-tetranitro-1,4,5,8-tetraazadecalin). *J Phys Chem*, 2006, B110: 10651–10661
35 Sun H. COMPASS: An *ab initio* force-field optimized for condensed-phase applications - Overview with details on alkane and benzene compounds. *J Phys Chem*, 1998, B102: 7338–7364
36 Hwang MJ, Stockfisch TP, Hagler AT. Derivation of class II force fields: 2. Derivation and characterization of a class-II force field, CFF93, for the alkyl functional group and alkane molecules. *J Am Chem Soc*, 1994, 116: 2515–2525
37 Maple JR, Hwang MJ, Stockfisch TP, Dinur U, Waldman M, Ewig CS, Hagler AT. Derivation of class-II force fields. 1. Methodology and quantum force-field for the alkyl functional group and alkane molecules. *J Comput Chem*, 1994, 15: 162–182
38 Lifson S, Hagler AT, Dauber P. Consistent force field studies of intermolecular forces in hydrogen-bonded crystals. 1. Carboxylic acids, amides, and the C=O···H Hydrogen bonds. *J Am Chem Soc*, 1979, 101: 5111–5121
39 Andersen HC. Molecular dynamics simulations at constant pressure and/or temperature. *J Chem Phys*, 1980, 72: 2384–2393
40 Parrinello M, Rahman A. Polymorphic transitions in single crystals: A new molecular dynamics method. *J Appl Phys*, 1981, 52: 7182–7190
41 Allen MP, Tildesley DJ. *Computer Simulation of Liquids*. Oxford: Oxford University Press, 1987
42 Politzer P, Murray JS, Lane P, Sjoberg P, Adolph HG. Shock-sensitivity relationships for nitramines and nitroaliphatics. *Chem Phys Lett*, 1991, 181:78–82